Journal of Solid State Chemistry 182 (2009) 2904–2911

Contents lists available at ScienceDirect

Journal of Solid State Chemistry

journal homepage: www.elsevier.com/locate/jssc

Locating redox couples in the layered sulfides with application to $Cu[Cr_2]S_4$

John B. Goodenough *, Youngsik Kim

Texas Materials Institute, University of Texas at Austin, 1 University Station C2201, Austin, TX 78712, USA

ARTICLE INFO

Article history:
Received 3 April 2009
Received in revised form
23 July 2009
Accepted 2 August 2009
Available online 7 August 2009

Keywords:
Li-ion battery
Layered sulfides
Redox-couple pinning
Ferromagnetic thiospinel

ABSTRACT

Use of $LiPF_6$ in EC:DEC as electrolyte has allowed electrochemical extraction of Li from $LiV_{1-y}M_yS_2$ and $LiTi_{1-y}M_yS_2$ (M = Cr or Fe). The data show access not only to the Ti(IV)/Ti(III) and V(IV)/V(III) redox couples, but also to the V(V)/V(IV) and Fe(III)/Fe(II) couples in these layered sulfides. However, the Cr(IV)/Cr(III) couple could not be accessed. The concept of redox-couple pinning is outlined and applied to the V(V)/V(IV) and Fe(III)/Fe(II) couples, which are pinned at the top of the *S*-3*p* bands. Holes associated with the "pinned" couples occupy orbitals of dominant *S*-3*p* character, but they have sufficient cation-3*d* character to prevent condensation of the holes into *p*–*p* antibonding states of disulfide bonds. Strong covalent bonding in the pinned couples creates itinerant-electron states in the partially occupied couples. Application to the metallic, ferromagnetic thiospinel $Cu[Cr_2]S_4$ favors location of the itinerant holes in states of a pinned Cu(II)/Cu(I) couple having primarily *S*-3*p* character.

1. Introduction

With the discovery [1] that reversible electrochemical extraction of Li from $LiVS_2$ is possible with $LiPF_6$ in ethylene/diethyl carbonate (EC/DEC) as electrolyte, we report a reinvestigation of electrochemical extraction of Li from $LiV_{1-y}M_yS_2$ and from $LiTi_{1-y}M_yS_2$ with M = Cr or Fe. The original studies [2–5] of these systems were frustrated by the irreversibility of electrochemical extraction of Li with $LiClO_4$ in propylene carbonate (PC) as electrolyte. Although these early authors were able to extract Li chemically with I_2/I^- in acetonitrile, the oxidation states of the atoms in the delithiated compounds has remained controversial. In particular, the possibility of oxidation of Cr(III) and Fe(II) in these layered sulfides and, by implication, in other sulfides, remains unresolved. Since these early studies, the concept of "pinning" of a redox couple at the top of anion-*p* bands has been proposed [6], and we use this concept not only to interpret our findings, but also to revisit an old controversy concerning the atomic oxidation states in the metallic, ferromagnetic spinel $Cu[Cr_2]S_4$.

2. Experimental methods

2.1. Synthesis

Polycrystalline nominal $LiM_yM'_{1-y}S_2$ (M or M' = Ti, V, Cr, Fe) were obtained from 2-g batches of Li_2S (Aldrich, ≥98.0%) and appropriate elements, Ti (Alfa, 99.9%), V (Alfa, 99.5%), Cr (Alfa, 99.95%), Fe (Alfa, 99.998%), and S (Aldrich, 99.99%). They were mixed, ground together, placed inside a pre-dried, carbon-coated quartz tube inside an Ar glove box, and then sealed under vacuum. The sealed tube was heated slowly over 20 h to 750 °C, held for 40 h, and then cooled to 250 °C over 10 h followed by quenching in air. The samples were removed to an Ar glove box where they were thoroughly ground and pelletized. Then they were treated again under the above process. Since these compounds are moisture-sensitive, they were always handled in an Ar atmosphere once they were removed to the glove box.

2.2. Electrochemical analysis

Since the samples are sensitive to moisture, the electrode disks and cells were prepared in the Ar glove box. The electrodes were fabricated from a 70:20:10 (wt%) mixture of active material:acetylene black as a current conductor:polytetrafluoroethylene (PTF). The active material and acetylene-black conductor were mixed completely first, the PTF binder was then added and then mass mixed again. The mixture was rolled into thin sheets and punched into 7-mm-diameter circular disks as electrodes. The typical electrode mass and thickness were 5–10 mg and 0.03–0.08 mm, respectively. The electrochemical cells were prepared in standard 2016 coin-cell hardware with lithium-metal foil as both the counter and reference electrodes. The electrolyte used for analysis was 1 M $LiPF_6$ in 1:1 ethylene carbonate/diethyl carbonate (EC/DEC). The sealed cells were taken out of the glove box and placed in a battery-testing system (Arbin BTS-2043); they were aged for 5 h before the first discharge (or charge) to ensure full absorption

* Corresponding author. Fax: +1 512 471 7681.
E-mail address: jgoodenough@mail.utexas.edu (J.B. Goodenough).

0022-4596/$ - see front matter © 2009 Elsevier Inc. All rights reserved.
doi:10.1016/j.jssc.2009.08.005

of the electrolyte into the electrode. A ten-minute rest period was employed between the charge and discharge steps.

3. Results

The XRD patterns of the $LiV_{1-y}M_yS_2$ and $LiTi_{1-y}M_yS_2$ (M = Cr, Fe) were all in good agreement with published data [4,5]. The hexagonal structure of the $LiV_{1-y}M_yS_2$ and $LiTi_{1-y}M_yS_2$ (M = Cr, Fe) consists of hexagonal-close-packed sulfur with M and Li atoms in alternate octahedral-site (001) planes. On removal of Li, the MS_2 layers are held together by van der Waals bonding. However, high-temperature synthesis commonly gives a ratio $Li/M < 1.0$ in the layered chalcogenide compounds [1,3]. The as-prepared samples in this work were also found to be slightly Li-deficient.

Fig. 1 shows the voltage profiles for the first 10 charge/discharge cycles of Li extraction from and intercalation into $Li_{1-x}V_{1-y}Cr_yS_2$. The as-prepared samples all tended to be deficient in Li, so the first charge (extraction of Li) had a smaller capacity than the subsequent charging curves for $y = 0$, 0.25, and 0.5. Fig. 2 shows the voltage profiles for the second charge of $Li_{1-x}V_{1-y}Cr_yS_2$. The small steps in the $y = 0$ voltage profile of Fig. 2 occur [1] in the compositional ranges of the different phases identified chemically by Murphy et al. [2] Addition of 0.25 Cr(III) for V(III) removes the steps in the voltage profile, increases the capacity, and raises the voltage further; but the capacity decreases with increasing y for $y \geq 0.5$. By $y = 0.75$, a flat $V(x)$ curve in the interval

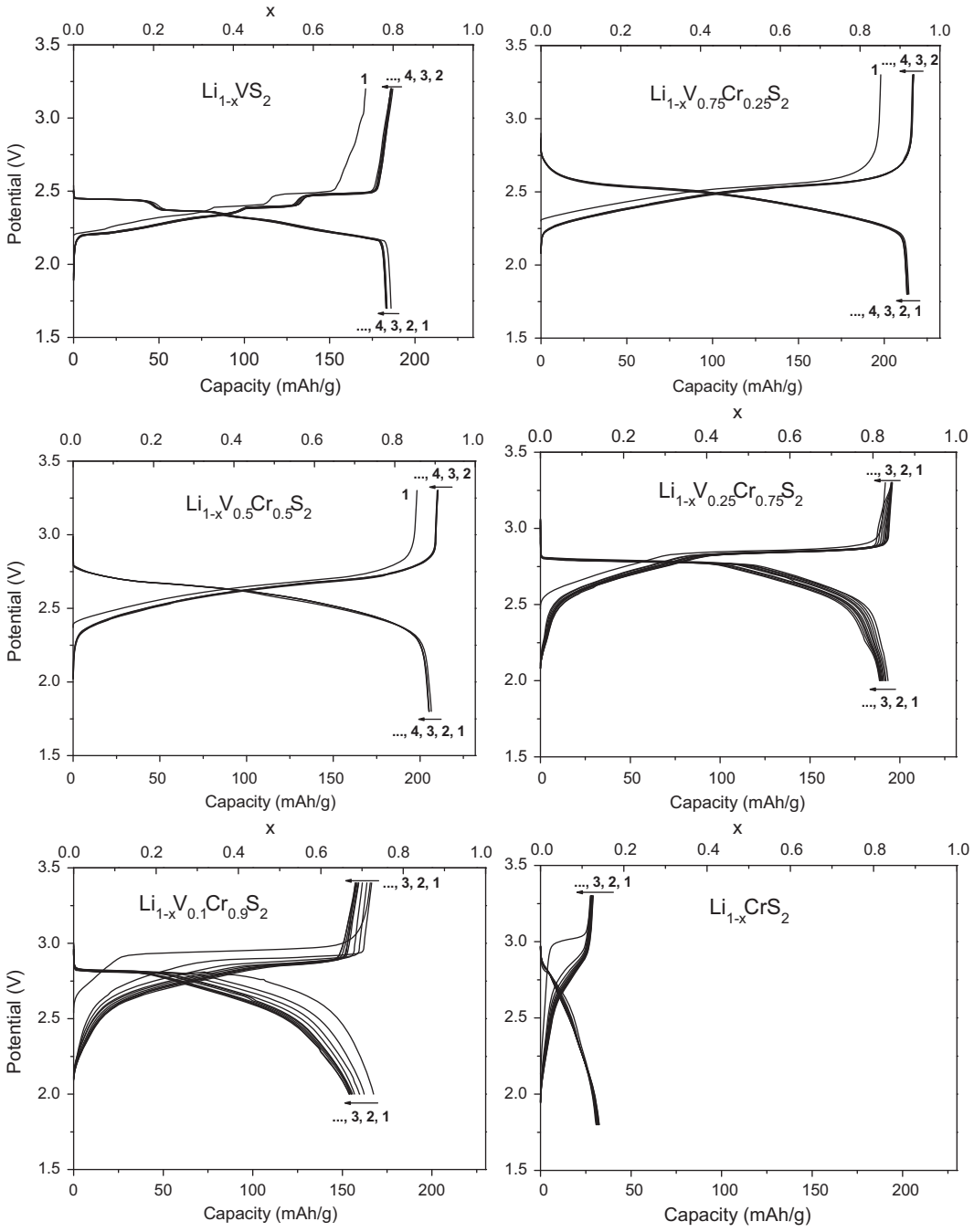

Fig. 1. The voltage profiles for the discharge and charge curves on cycling of Li intercalation into $Li_{1-x}V_{1-y}Cr_yS_2$ at the rate of 0.1 mA/cm^2.

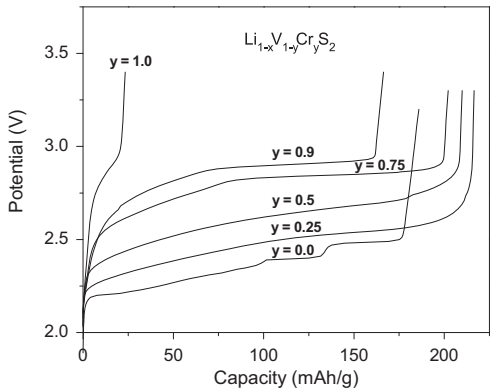

Fig. 2. The voltage profiles for the second-charge curves on Li extraction from $Li_{1-x}V_{1-y}Cr_yS_2$.

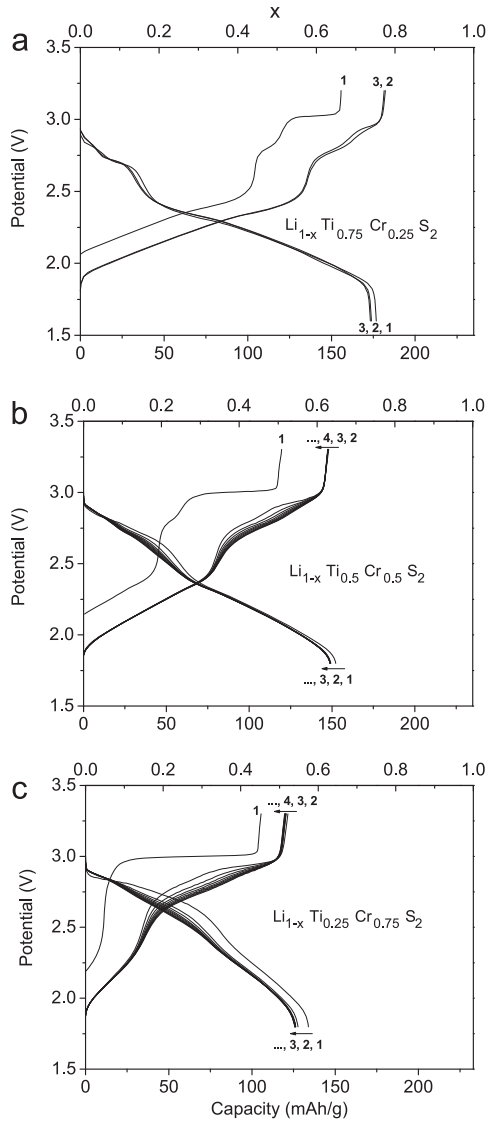

Fig. 3. The voltage profiles for the discharge and charge curves on cycling of Li intercalation into $Li_{1-x}Ti_{1-y}Cr_yS_2$ at the rate of 0.1 mA/cm^2.

$0.4<x<0.8$ signals an irreversible decomposition as the voltage approaches 2.8 V versus Li^+/Li^0. It was not possible to oxidize Cr(III) by extracting Li electrochemically from $LiCrS_2$. However, a capacity corresponding to $0\le x<1$ in $LiV_{0.5}Cr_{0.5}S_2$ indicates that the V(V)/V(IV) in addition to the V(IV)/V(III) couple is accessible. The V(V)/V(IV) couple is pinned at the top of the *S*-3*p* bands whereas the Cr(IV)/Cr(III) couple lies too far below the top of the *S*-3*p* bands to permit the introduction of a significant concentration of holes into the *S*-3*p* bands.

DiSalvo et al. [5] have reported chemical removal of Li from $LiV_{1-y}Cr_yS_2$ with I_2/I^- in acetonitrile. They observed little change of the lattice parameters from those of VS_2 in the range $0\le y\le 0.5$; they reported no lattice parameters for CrS_2, which implies that complete topotactic chemical extraction of Li from compositions with $0.5<y\le 1.0$ was not possible. These authors also reported the magnetic susceptibility below 300 K only for $y=0.50$ and 0.75 of $V_{1-y}Cr_yS_2$. Their unusual magnetic data can be interpreted to be a susceptibility below a T_N of the Cr(III) in *ca.* V(V)Cr(III)S_4 with a Cr-rich paramagnetic phase giving the apparent "turn on of a paramagnetic susceptibility" from a second phase. Therefore, we conclude that chemical extraction of Li from $LiV_{1-y}Cr_yS_2$ also provides little evidence of oxidation of Cr(III) in the layered sulfides.

As a further check of this conclusion, we have investigated $Li_{1-x}Ti_{1-y}Cr_yS_2$. Fig. 3 shows the voltage profiles versus Li^+/Li^0 for $y=0.25$, 0.5, 0.75. The curve for $LiTiS_2$ is similar to that originally reported by Whittingham [7]. The $y=0.5$ sample shows a step at $x\approx 0.2$ in the first charge and a plateau near $V\approx 3.0$ V. On subsequent cycles, the plateau near 3.0 V decreases until the charge/discharge cycle becomes reversible. This unusual behavior appears to be associated with the Cr atoms, which suggests access to *S*-3*p* antibonding states associated with the Cr(IV)/Cr(III) couple in the presence of Ti(IV). Holes introduced into the *S*-3*p* bands at $V=3.0$ V cause some decomposition as is evidenced by the irreversibility of the initial charge/discharge cycles in the range $2.4<V<3.0$ V. In $LiCrS_2$, however, oxidation of the *S*-3*p* bands is limited; without Ti neighbor, the Cr(IV)/Cr(III) couples have little influence on the concentration of itinerant holes that can be supported in the *S*-3*p* bands of $LiCrS_2$(Fig. 1).

Murphy et al. [4] have shown that $LiV_{1-y}Fe_yS_2$ can be prepared for $y\le 0.5$. Our voltage profiles for $y=0.1$, 0.25, and 0.5 are shown in Fig. 4. The evolution with y of the second-charge profile is shown in Fig. 5. In contrast to the $y=0$ profile, the introduction of Fe, like the introduction of Cr, eliminates some of the intermediate phases of the $Li_{1-x}VS_2$ profile and allows a more complete extraction of Li. Moreover, the introduction of 0.1 and 0.25 Fe transforms the voltage profiles into two plateaus with a step at $x=0.5$, which is suggestive of an intermediate phase having ordered Li^+ ions at $x=0.5$. On the second charge, nearly all of the Li can be extracted reversibly for $y=0.1$ and 0.25, but with a capacity fade on subsequent cycles of the $y=0.25$ sample. The behavior of the $y=0.5$ sample is similar to that of the $y=0.25$ sample; but in the range $0.5<x<1.0$, the plateau is replaced by a range of Li solid solution. These data are compatible with an Fe(III)/Fe(II) couple that overlaps the V(V)/V(III) couple pinned at the top of the *S*-3*p* bands. A reversible extraction of Li to $x=0.9$ in the $y=0.5$ sample requires access to the Fe(III)/Fe(II) couple with $V(V)_{0.5}Fe(III)_{0.5}S_2$ at $x=1.0$. The existence of the spinel Fe_3S_4, but not of Fe_2S_3, shows that partial oxidation of Fe(II) is possible in a sulfide; the capacity fade of the $y=0.25$ and 0.5 samples on cycling to $x=1$ may be due to the dominant *S*-3*p* character of the empty antibonding states at octahedral-site V(V) and Fe(III) ions in sulfides. Jacobson and McCandlish [8] have demonstrated with Mössbauer data the existence of tetrahedral-site Fe(III) in $KFeS_2$. Finally, magnetic susceptibility measurements of DiSalvo et al. [5] have shown that the Fe(III)/Fe(II) couple is in a low-spin state with a large *S*-3*p* component in the antibonding states associated with the Fe(III) ions of the $y=0.5$ sample.

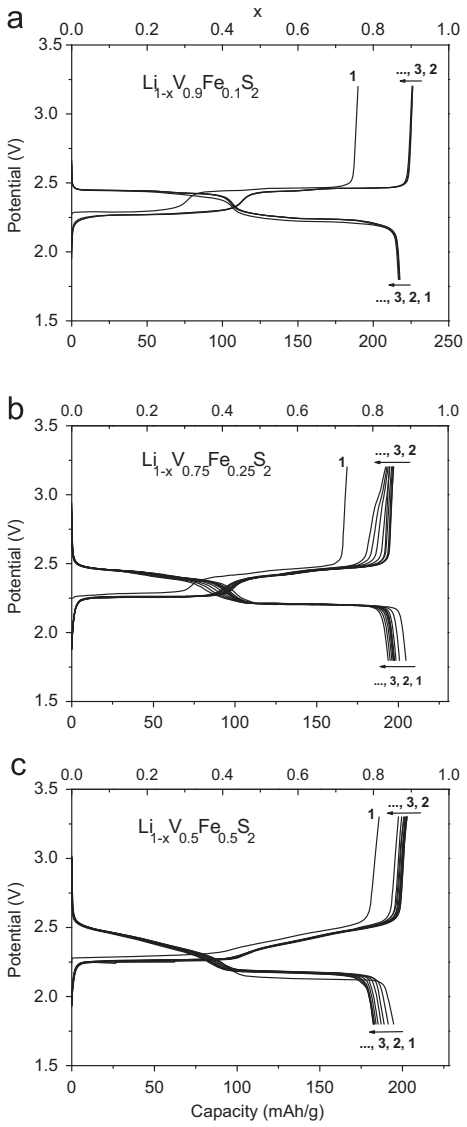

Fig. 4. The voltage profiles for the discharge and charge curves on cycling of Li intercalation into the $Li_{1-x}V_{1-y}Fe_yS_2$ at the rate of 0.1 mA/cm^2.

Tarascon et al. [9] have reported preparation of nominal $LiTi_{1-y}Fe_yS_2$ for all values of y and the total removal of Li for $y = 0.10$ and 0.25. Mössbauer data showed an isomer shift (IS) for the Fe(II) spectra near 0.8 mm/s, characteristic of high-spin Fe(II) in sulfide octahedral sites [10] for all $y \leq 0.5$; but for $y \geq 0.5$, a change to more than two lines appeared, indicating the presence of low-spin Fe(III). On removal of Li from the $y = 0.1$ sample, their paramagnetic susceptibility data showed a progressive transition to a low-spin iron by $x = 0.8$ where all the titanium would be changed to Ti(IV) before oxidation of Fe(II). Similarly, removal of Li from the $y = 0.25$ sample showed an abrupt drop in the IS at $x = 0.5$ where all the titanium would be Ti(IV) and further removal of Li would create Fe(III). Fig. 6 shows our voltage profile for $Li_{1-x}Ti_{0.5}Fe_{0.5}S_2$. A reversible extraction of nearly 0.5 Li/f.u. shows that the Fe(III) state is accessed, but the profile also shows an instability associated with the introduction of holes into the *S*-3*p* bands. All these data for the $Li_{1-x}Ti_{1-y}Fe_yS_2$ system are consistent with a pinning of the Fe(III)/Fe(II) couple at the top of the *S*-3*p* bands with an overlap of the bottom of the itinerant 3*d* band of the Ti(IV)/Ti(III) couple.

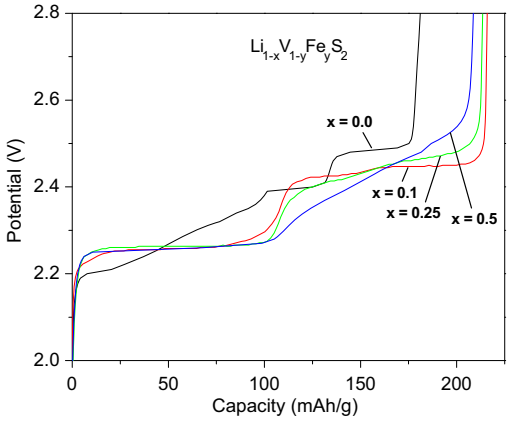

Fig. 5. The voltage profiles for the second-charge curves on Li extraction from $Li_{1-x}V_{1-y}Fe_yS_2$.

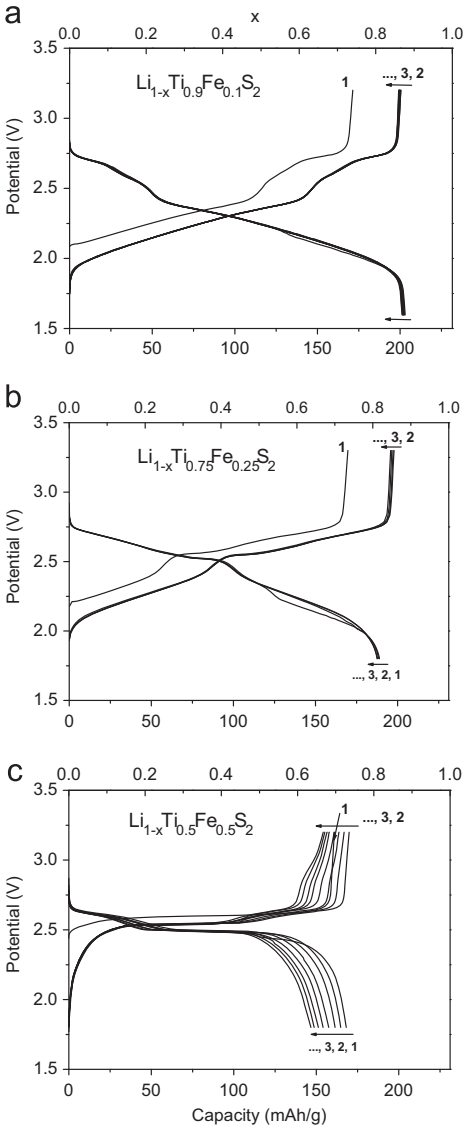

Fig. 6. The voltage profiles for the discharge and charge curves on cycling on Li intercalation into $Li_{1-x}Ti_{1-y}Fe_yS_2$ at the rate of 0.1 mA/cm^2.

4. Discussion

Redox-couple pinning illustrates but one way that nature stabilizes occupied states at the expense of empty states. The concept of redox-couple pinning is illustrated schematically in Fig. 7 where we show the states of a d^n/d^{n+1} redox couple as it moves from above to below the top of an anion-p band. Where the cation redox couple lies above the p bands, the antibonding states have a predominantly d-orbital character, but covalent admixture of p states raises the energy of the empty states of a couple relative to the occupied states. Therefore, we label the hole states as $(d+p)^n$. As the couple approaches the top of the anion-p bands, the covalent mixing becomes strong enough to broaden a partially occupied couple into a band of itinerant states. Hybridization also lowers a corresponding manifold of predominantly anion-p states, which is not shown. At crossover, the empty antibonding states of a partially occupied couple change from predominantly cation-3d to predominantly anion-p in character, marked *a.b.*: $(p+d)^n$, and the occupied bonding d^{n+1} states, marked *b.*: $(d+p)^{n+1}$, fall below the top of the anion-p bands. The symmetry of the hole orbitals is not changed by this crossover, which allows identification of the antibonding hole states with the redox couple even though they are predominantly anion-p states. However, as the redox couple falls further below the top of the anion-p bands, fewer antibonding states associated with the redox couple are raised above the top of the anion-p bands and the holes occupy nearly

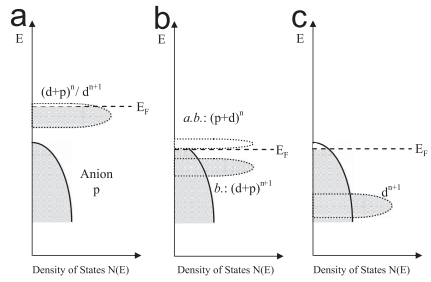

Fig. 7. Schematic representation of a slightly oxidized redox couple as it passes through the top of the anion-p bands: (a) itinerant versus polaronic character of hole states of couple on the approach to the top of anion-p band, (b) pinned couple with predominantly antibonding (*a.b.*) anion-p hole states and predominantly cation-d bonding (*b.*) states, (c) couple too far below top of anion-p band for significant cation-d character in hole states.

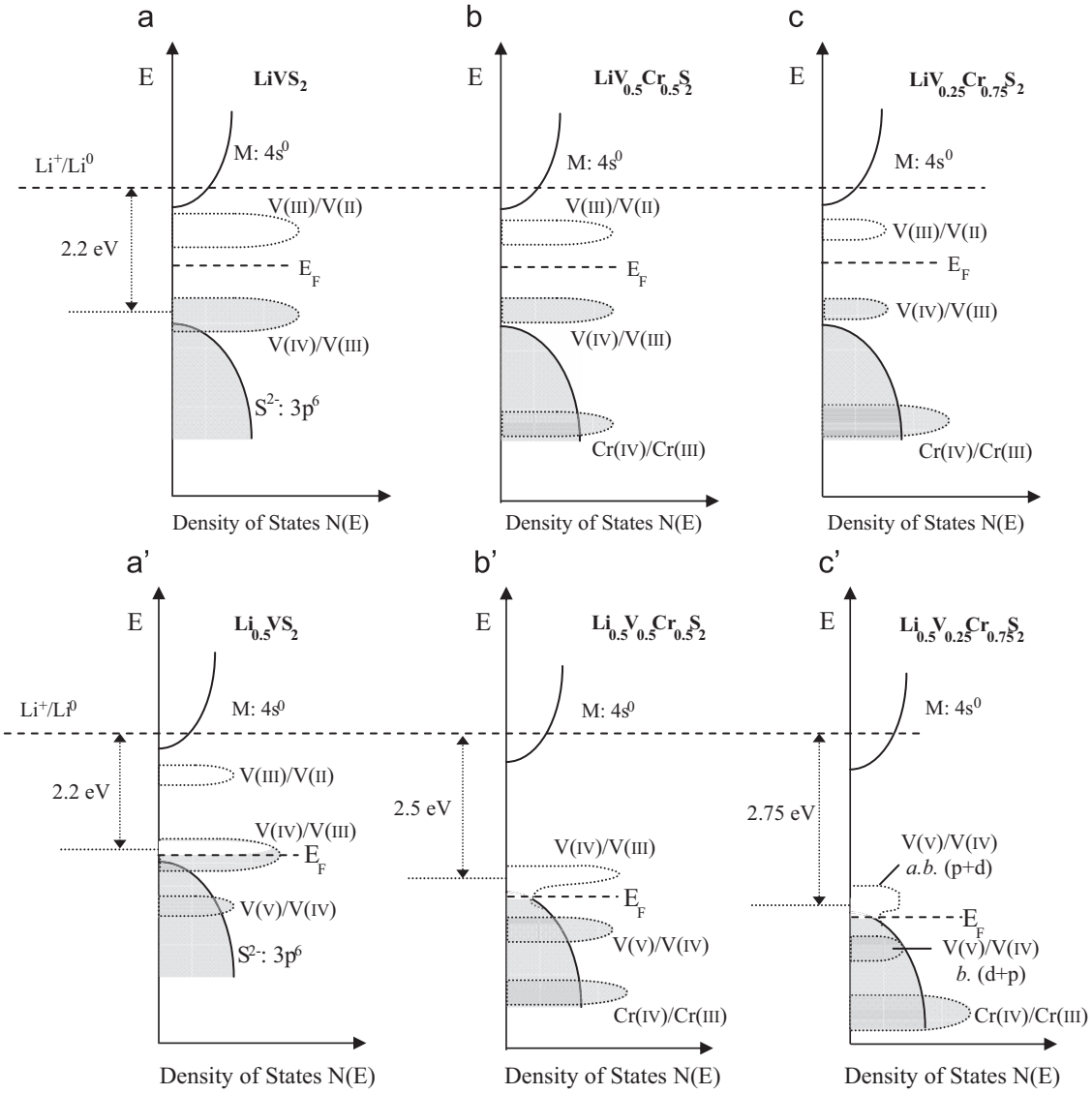

Fig. 8. Positions of the V(IV)/V(III), V(V)/V(IV), and Cr(IV)/Cr(III) redox couples relative to the Fermi energy of lithium in the layered $Li_{1-x}V_{1-y}Cr_yS_2$ sulfides.

pure anion-*p* states; at larger concentration, these anion-*p* holes condense into dianion *p*–*p* antibonding states.

Fig. 8 shows a schematic energy diagram for $Li_{1-x}V_{1-y}Cr_yS_2$ with $x = 0$, 0.5 and $y = 0$, 0.5, 0.75. The bottom of the Cr-4s^0 band is at a lower energy than that of the V-4s^0 band [9], which in turn lowers somewhat the top of the *S*-3*p* band. Not shown is the position of the empty Cr(III)/Cr(II) level, which lies above the bottom of the 4s^0 band as do the Li:2s^0 states. Similarly, Fig. 9 shows the $Li_{1-x}V_{1-y}Fe_yS_2$ energies for $x = 0$, 0.5 and $y = 0$, 0.25, 0.5. Fig. 10 represents $Li_{1-x}Ti_{1-y}Cr_yS_2$ with $x = 0$, 0.5 and $y = 0$, 0.5, 0.75; Fig. 11 represents $Li_{1-x}Ti_{1-y}Fe_yS_2$ with $x = 0$, 0.5 and $y = 0$, 0.25, 0.5. These figures illustrate pinning of the V(V)/V(IV), and Fe(III)/Fe(II) couples at the top of the 3*p* bands and placement of the Cr(III)/Cr(II) level too far below the top of the *S*-3*p* bands for oxidation of the Cr(IV)/Cr(III) couple.

4.1. Application to the spinel $Cu[Cr_2]S_4$

In 1964, Lotgering [11] reported the interesting finding that the thiospinel $Cu[Cr_2]S_4$ is a ferromagnetic metal with a magnetization at $T = 0$ K of 5 μ_B/f.u. Interpretation of this finding depends on placement of the Cu(II)/Cu(I) and Cr(IV)/Cr(III) redox couples relative to the top of the *S*-3*p* bands. Lotgering [12] noted that Cu(II) is generally not accessible in chalcogenides and argued for the presence of Cr(IV)/Cr(III) and Cu(I) in spite of the fact that the oxospinel $Cu[Cr_2]O_4$ was known [13] to contain Cu(II) and Cr(III). From a knowledge of the valences of the oxospinel, Goodenough [14] argued for the presence of Cu(II), but with sufficiently strong covalent bonding with the *S*-3*p* orbitals that the holes of *d*-like symmetry at the Cu(II) are itinerant. Lotgering and Van Stapele [15] pointed out that placement of both the Cu(II)/Cu(I) and the Cr(IV)/Cr(III) couples below the top of the *S*-3*p* bands would mean the itinerant holes occupy the *S*-3*p* bands, and this suggestion was later claimed to be established [16–18]. However, if the holes are only in *S*-3*p* bands, we should expect them to be trapped in disulfide bonds of $(S_2)^{2-}$ as occurs in the disproportionation of Fe_2S_3 into FeS and $Fe(S_2)$. The fact that such a disproportionation is not found in $Li_{0.5}Ti_{0.5}Fe_{0.5}S_2$ signals that, in this sulfide, the Fe(III)/Fe(II) couple lies closer to the top of the *S*-3*p* bands than in FeS, which gives a stronger pinning of the couple. In addition, placement of holes only in the *S*-3*p* bands of $Cu[Cr_2]S_4$ would call for a magnetization in excess of 6 μ_B/f.u. since the localized Cr(III):t^3 configurations should induce parallel spins on the sulfur array. Therefore, we need to invoke "pinning" of either the Cu(II)/Cu(I) or the Cr(IV)/Cr(III) couple at the top of the *S*-3*p* bands.

Comparison of the voltage profiles of $Li_{1-x}TiS_2$ and the spinel $Li_{2-x}[Ti_2]S_4$ shows they are essentially identical; [19,20] in the

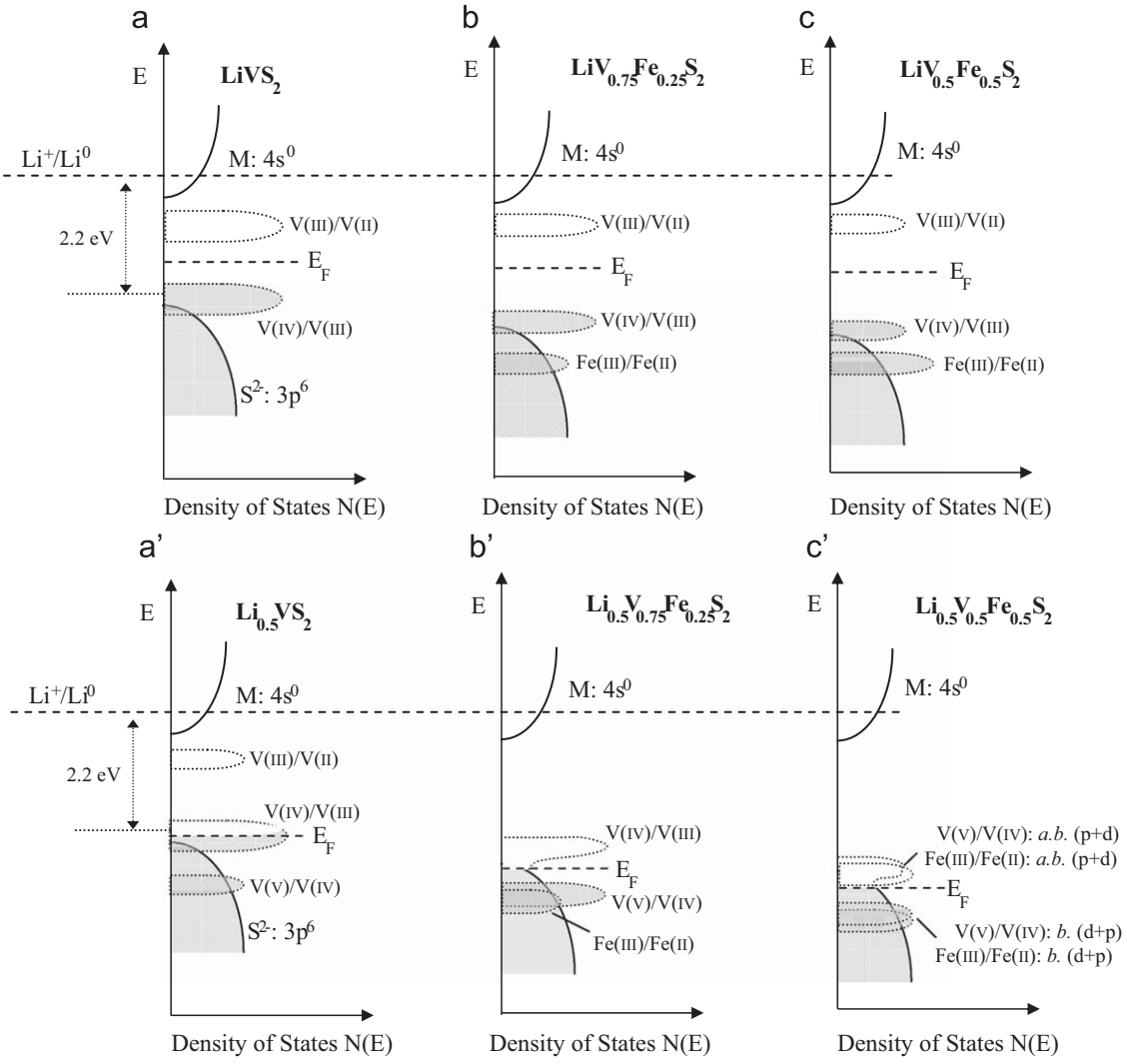

Fig. 9. Positions of the V(IV)/V(III), V(V)/V(IV), and Fe(III)/Fe(II) redox couples relative to the Fermi energy of lithium in the layered $Li_{1-x}V_{1-y}Fe_yS_2$ sulfides.

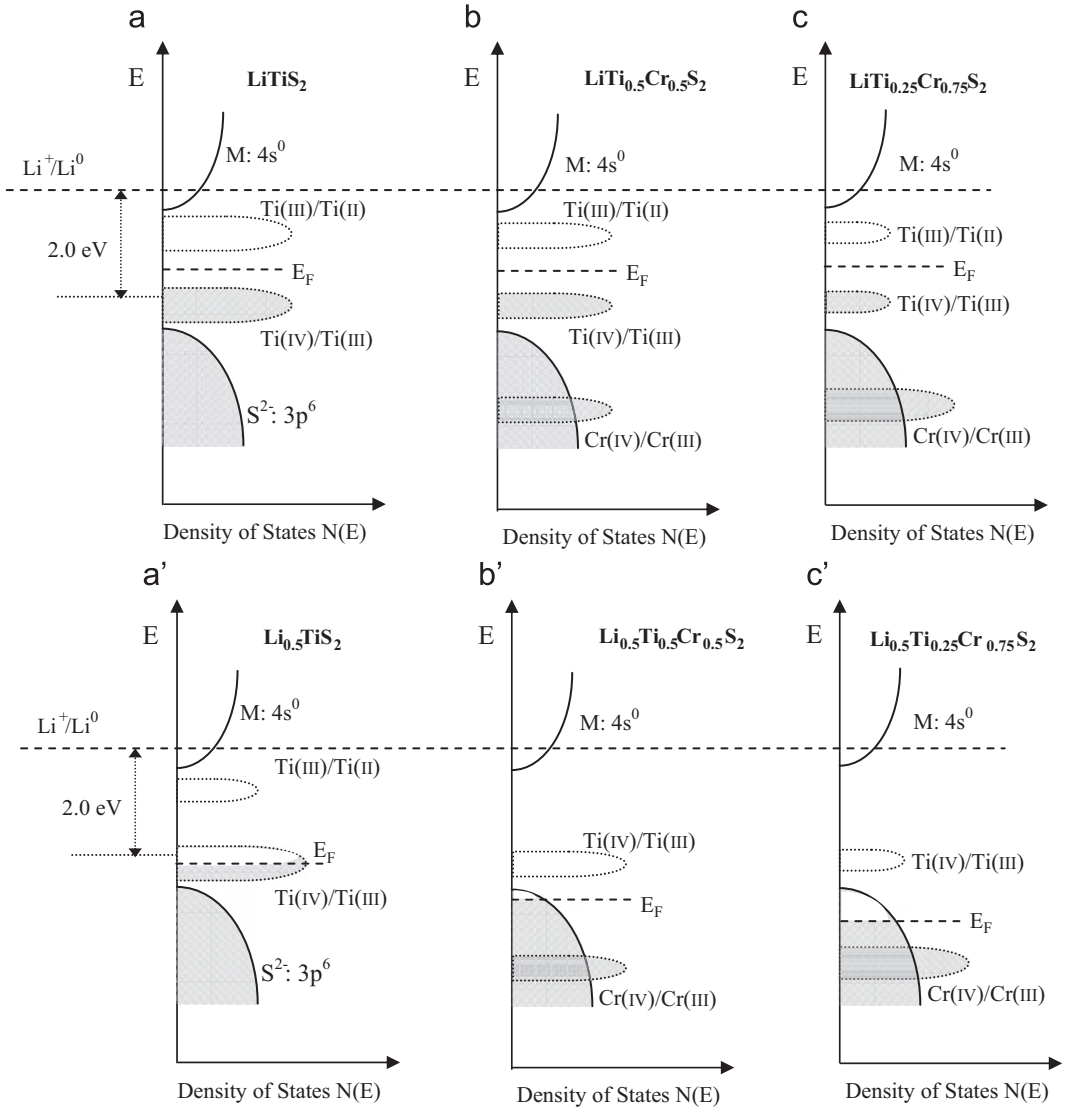

Fig. 10. Positions of the Ti(IV)/Ti(III), Cr(IV)/Cr(III) redox couples relative to the Fermi energy of lithium in the layered $Li_{1-x}Ti_{1-y}Cr_yS_2$ sulfides.

thiospinel $[Ti_2]S_4$ framework, as in the layered sulfide, the Li^+ ions occupy only octahedral sites. Therefore, we can expect the Cr(IV)/Cr(III) couple in $Cu[Cr_2]S_4$ to lie relative to the top of the *S*-3*p* bands as in $LiCrS_2$; and our data for $Li_{1-x}Ti_{1-y}Cr_yS_2$ clearly show that the Cr(IV)/Cr(III) couple in the layered sulfide $LiCrS_2$ lies too low in energy to be pinned at the top of the *S*-3*p* bands. Moreover, covellite has a structure that corresponds to $Cu(I)_2(S_2)\cdot CuS$ in which two Cu(I) occupy tetrahedral sites, one Cu(II) occupies a square-coplanar site, and *S*–*S* pairs coexist with isolated S atoms. Since there is no reason why the relative energies of $Cu[Cr_2]O_4$ should become inverted in $Cu[Cr_2]S_4$, we believe we can say unequivocally that the Cu(II)/Cu(I) couple is what is primarily pinned at the top of the *S*-3*p* bands in the thiospinel $Cu[Cr_2]S_4$. However, it is to be emphasized that the holes occupy states that are predominantly *S*-3*p* in character; it is therefore difficult to distinguish experimentally these pinned Cu(II)/Cu(I) (*p*–*d*) hybridized antibonding states from *S*-3*p* band states. Bodenez et al. [18] clearly establish the retention of Cr(III) in $Cu[Cr_2]S_4$ and they claim to observe some shorter *S*–*S* bonds, but the metallic conductivity of $Cu[Cr_2]S_4$ shows that the holes in the *S*-3*p* bands are not trapped out at disulfide anions. Hybridization with Cu-3*d* to create antibonding states at the top of the *S*-3*p* bands can account for the antiferromagnetic coupling of the *S*-3*p* electrons and the localized Cr(III):t^3 spins, the lack of capture of the holes in $(S_2)^{2-}$ ions, and the presence of a small paramagnetic spin of the Cu sites observed by Kimura et al. [21] with magnetic circular dichroism.

5. Conclusions

Li extractions from $LiV_{1-y}M_yS_2$ and from $LiTi_{1-y}M_yS_2$ (M = Cr or Fe) with $LiPF_6$ in EC:DEC as the electrolyte have revealed access to the Fe(III)/Fe(II) couple pinned at the top of the *S*-3*p* bands, but not to the Cr(IV)/Cr(III) couple. The V(IV)/V(III) and V(V)/V(IV) couples are also pinned with a change in the character of the hole states on oxidation from primarily V-3*d* in the V(IV)/V(III) couple to primarily *S*-3*p* in the V(V)/V(IV) couple. Application of these findings to the long-standing controversy over the valence states in the thiospinel $Cu[Cr_2]S_4$ favors a pinning of the Cu(II)/Cu(I) couple at the top of the *S*-3*p* bands with a dominant *S*-3*p* character in the hole states, but with a sufficient Cu-3*d* character to give conduction electrons with

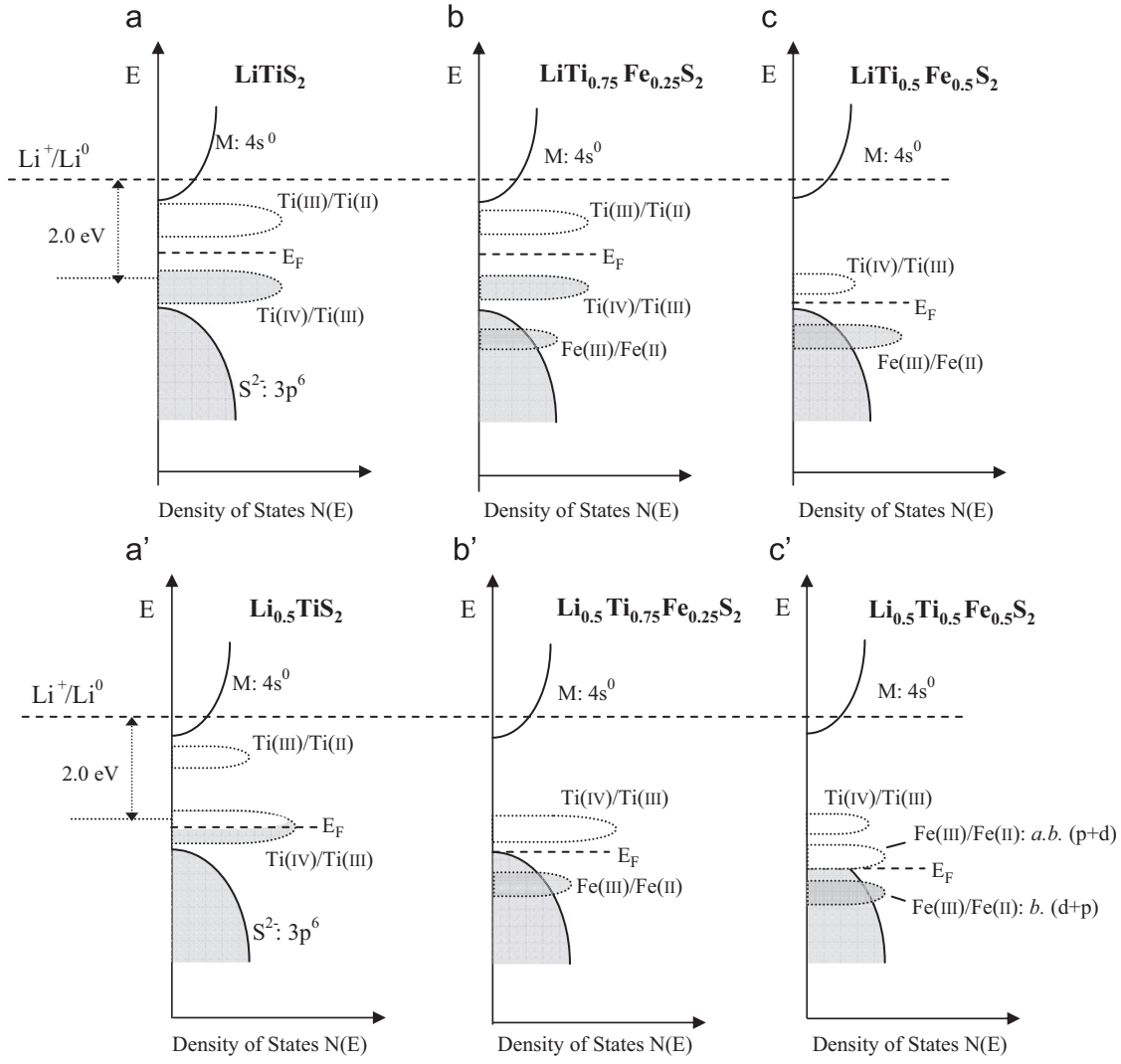

Fig. 11. Positions of the Ti(IV)/Ti(III), Fe(III)/Fe(II) couples relative to the Fermi energy of lithium in the layered $Li_{1-x}Ti_{1-y}Fe_yS_2$ sulfides.

spins antiparallel to the localized Cu(III):t^3 spins at an energy well below the top of the *S*-3*p* bands.

Acknowledgments

This work was supported by the office of FreedomCAR and Vehicle Technologies of the US Department of Energy under Contract no. DE-AC03-76SF00098 and the Robert A. Welch Foundation of Houston, TX (Grant no. F-1066).

References

[1] Y.S. Kim, J.B. Goodenough, Electrochem. Solid State Lett. 12 (2009) A73.
[2] D.W. Murphy, J.N. Clarides, F.J. DiSalvo, C. Cros, J.V. Waszczak, Mater. Res. Bull. 12 (1977) 825.
[3] D.W. Murphy, J.N. Clarides, J. Electrochem. Soc. 126 (1979) 349.
[4] D.W. Murphy, F.J. DiSalvo, J.N. Clarides, J. Solid State Chem. 29 (1979) 339.
[5] F.J. DiSalvo, M. Eibshutz, C. Cros, D.W. Murphy, J.V. Waszczak, Phys. Rev. B 19 (1979) 3441.
[6] J.B. Goodenough, in: W.A. van Schalkwijk, B. Scrosati (Eds.), Advances in Lithium Batteries, Kluwer Academic/Plenum Publishers, New York, 2002, p. 135.
[7] M.S. Whittingham, Science 192 (1976) 1126.
[8] A.J. Jacobson, L.E. McCandlish, J. Solid State Chem. 29 (1979) 355.
[9] J.M. Tarascon, F.J. DiSalvo, M. Eibshutz, D.W. Murphy, J.V. Waszczak, Phys. Rev. B 28 (1983) 6397.
[10] J.B. Goodenough, G.A. Fatseas, J. Solid State Chem. 41 (1982) 1.
[11] F.K.Lotgering, in: Proceedings of the International Conference on Magnetism, Nottingham, 1964, p. 533.
[12] F.K. Lotgering, Solid State Commun. 2 (1964) 55.
[13] J.B. Goodenough, J. Phys. Soc. Japan 17 (B-1) (1962) 185.
[14] J.B. Goodenough, Solid State Commun. 5 (1967) 577.
[15] F.K. Lotgering, R.P. van Stapele, Solid State Commun. 5 (1967) 143.
[16] O. Yamashita, Y Yamaguchi, I. Nakatani, H. Watanabe, K. Matsumoto, J. Phys. Soc. Japan 46 (1979) 1145.
[17] R. Schöllhorn, Angew. Chem., Int. Ed. Engl. 27 (1988) 1392.
[18] V. Bodenez, C. Dupont, L. Laffont, A.R. Armstrong, K.M. Shaju, P.G. Bruce, J.M. Tarascon, J. Mater. Chem. 17 (2007) 3238.
[19] S. Sinha, D.W. Murphy, Solid State Ionics 20 (1986) 8.
[20] A.C.W.P. James, J.B. Goodenough, Solid State Ionics 27 (1988) 37.
[21] A. Kimura, J. Matsumo, J. Okabayashi, A. Fujimori, T. Shishidou, E. Kulatov, T. Kanomata, J. Electron. Spectrosc. Relat. Phenom. 114–116 (2001) 789.